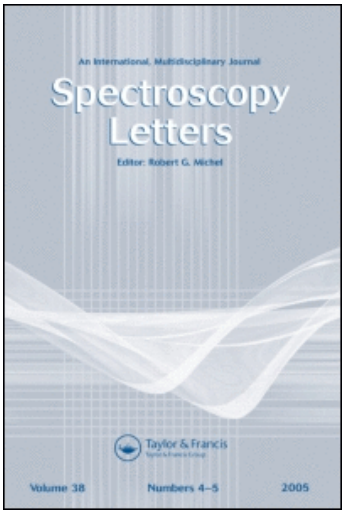

Spectroscopy Letters
Publication details, including instructions for authors and subscription information:
http://www.informaworld.com/smpp/title~content=t713597299

Far-Infrared of the Local Anesthetic Procaine

M. Alcolea Palafox[a]
[a] Departamento de Quimica-Fisica I (Espectroscopia), Facultad de Ciencias Quimicas, Universidad Complutense, Madrid, Spain

To cite this Article Palafox, M. Alcolea(1997) 'Far-Infrared of the Local Anesthetic Procaine', Spectroscopy Letters, 30: 8, 1495 — 1514
To link to this Article: DOI: 10.1080/00387019708006740
URL: http://dx.doi.org/10.1080/00387019708006740

SPECTROSCOPY LETTERS, 30(8), 1495-1514 (1997)

FAR-INFRARED OF THE LOCAL ANESTHETIC PROCAINE

Key words: Far infrared, amino group, AM1, procaine, local anesthetics

M. Alcolea Palafox

Departamento de Química-Física I (Espectroscopia), Facultad de Ciencias Químicas, Universidad Complutense, 28040-Madrid, Spain

ABSTRACT

The low spectral region of procaine was studied by far-infrared spectroscopy. Raman lines were registered and interpreted. An equivalent study was performed on the molecule of benzocaine. In the characterization of the bands, and in the description of the torsion-inversion mode of the *p*-amino group, the AM1 semiempirical method was used. The optimum geometry parameters, the torsion and inversion potential functions, the energy levels, and the transitions were obtained. The effects of temperature on the torsion and inversion modes were studied.

INTRODUCTION

The far-infrared (FTIR) vapour phase spectrum of aniline[1,2] and substituted anilines are dominated by transitions between the inversion energy levels of the amino group. In the solid state, however, the search for such experimental inversion frequencies is more complicated, because these bands appear very broad and with weak intensity.

Among aniline derivatives, the amino group of several local anesthetics has been reported to have an importance influence on anesthetic action[3-6]. The

molecules of benzocaine (BEN) and procaine (PRC) of free basis, selected in the present study, are the first members of homologous series of higher local anaesthetics with multiple pharmaceutical applications. In these compounds, the *p*-amino group (NH_2 or ND_2) has two modes, torsion and inversion, in the low frequency range. In inversion, several transitions were identified in FTIR and are described in the present manuscript. As for torsion, the *p*-amino group can be considered symmetric with regard to the main axis of the molecule. Thus, there are two equivalent positions in a total rotation. The C_2 symmetry obtained gives a torsional band prohibited by IR selection rules. However, torsional bands were detected in the spectra of these compounds[7], as in aniline or halogenated derivatives[2]. This was interpreted[8] on the basis that the bands observed in the spectra are combinations between the torsion and inversion vibrations (transit 0–1), which are active in the infrared. Thus the torsion and inversion potential function of the *p*-amino group was studied separately in a previous work[9]. The present study considers both motions conjointly, obtaining a pathway of minimum energy. The potential energy barrier to the inversion is of interest, because its height must be related to the electron distribution on the amino nitrogen and in the benzene ring and to the nonplanarity of the amino fragment. Thus one of the objectives of the present study was to provide a tentative assignment of the torsion and wagging bands using high-resolution FTIR spectra.

EXPERIMENTAL

Samples of procaine and benzocaine of free basis were from MERCK and were used without further purification.

High-density polyethylene (MERCK), was used as the sample matrix and in the form of a solid solution. In the case of polyethylene as a matrix, the procedure was as follows: The powdered solid sample (≈ 5 mg) was mixed with 300 mg of polyethylene to produce a homogeneous mixture. The mixture was then compressed, yielding pellets 25 mm in diameter with non-plane surfaces and only slightly tidy, to avoid noise produced by interferences from parallel faces.

By heating the pellet until it becomes transparent (≈ 110 °C), the sample is taken up in the polyethylene matrix, yielding a solid solution. Keeping the pellet in the transparent state for a few seconds is usually enought to obtain a solid solution to the desired concentration. The reduction in optical transmittance should be in the range of 3000-4000 digital voltimeter units.

The Fourier Transform spectrometer used was a POLYTEC FIR30 with a GOLAY (Pye Unicam IR 50) detector with an optimum temperature of 300 K. The spectra were taken from 20 to 230 cm^{-1} with an apodized spectral resolution of 0.25 cm^{-1}; the range of our spectrometer system did not extend above 675 cm^{-1}, though the signal-to-noise ratio at the extreme ends of the range was not always good. Interferometer operation and data acquisition and processing was performed with a Hewlett-Packard instrument controller.

Raman spectra for samples were recorded on special glass U-cells using a Jobin-Yvon laser Raman spectrophotometer, model Ramanor U-1000 with double monochromator and

holographic gratings and a photon counter detector. The source was a 2 ω Spectra- Physics, model 165 Argon ion laser. Laser power was in the range 100-400 mω. The resolution was 1 cm^{-1}; band positions were accurate to ± 0.5 cm^{-1}. A Krypton ion laser was also used.

COMPUTATIONAL METHODS

Calculations were carried out using the standard AM1 procedure as implemented in the AMPAC package of computer programs[10,11], indicated for analyzing problems of molecular structure and reaction mechanisms.

The AMPAC package was used in its VAX/IV2 version with standard parameters. Only the AM1 method was utilized. All the geometry was optimized by minimizing energy with respect to all geometrical variables without imposing molecular symmetry constraints. The GAUSSIAN 92 package was also used[12].

The Figures were prepared on a Macintosh microcomputer using the BALL and STICK program[13].

RESULTS AND DISCUSSION

Low-frequency vibrations and spectra: The reference interferogram used between 10 and 650 cm^{-1} is shown in Fig 2. The FTIR spectrum of PRC in that spectral region is illustrated in Fig. 3. A summary of the assignments and numerical values for the observed band positions in the spectra are given in Table 1, columns fourth and sixth. The vibrational frequencies and intensities computed by AM1 in two conformations are listed in the first and second columns. The values in parentheses in the first column are for a less stable conformation. The relative intensity data in the second column were calculated by dividing the value obtained in each case by the intensity of the strongest line computed in the 10-700 cm^{-1} range. The scaled frequencies in the third column were calculated using the scale factors for liquid benzene or solid *p*-aminobenzoic acid[14].

Several of the lines observed in the FTIR spectrum in Fig. 3 represent various inversion transitions in the *p*-amino group. The inversion vibration (analogous to the "umbrella" vibration of ammonia) involves the motion of the two hydrogens through the plane, with simultaneous inversion of the nitrogen's lone pair of electrons. Because there are two equivalent equilibrium conformations, the potential energy curve for this vibration has a double minimum. Since the nitrogen's lone pair is partially conju-gated with the aromatic ring, both the equili-brium out-of-plane angle and the magnitude of the barrier separating these two minima are affected considerably by the presence of substituents on the ring, their electron withdrawing, donating, or polarizing ability, and their location relative to the amino group.

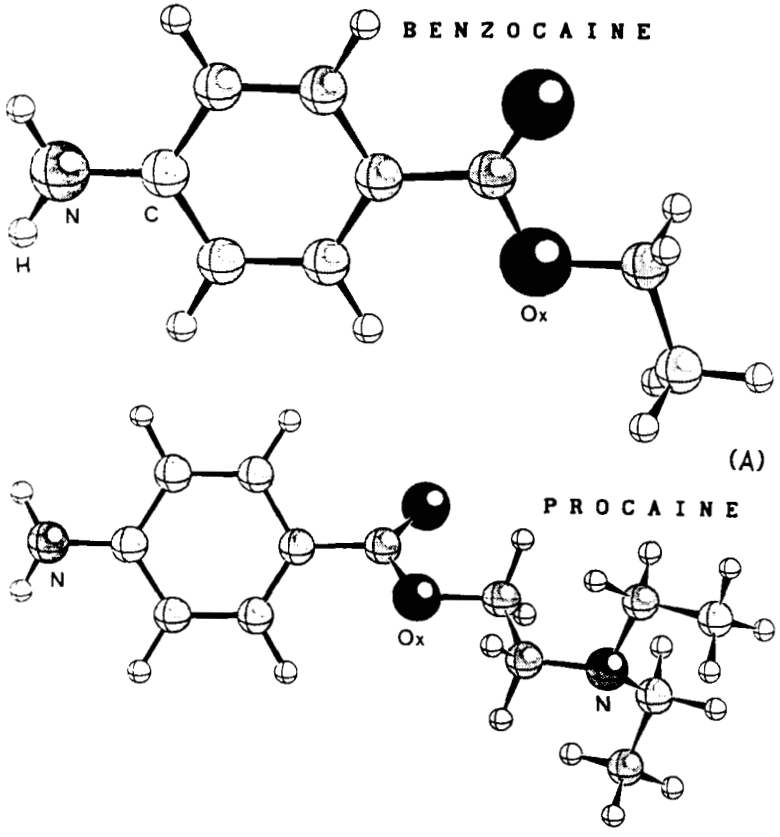

Fig. 1. Optimum geometries calculated for the molecules studied.

The energy levels of the inversion vibration may be deduced from the transitions between them, some being identified as intense absorption lines in the far-infrared spectrum. The results obtained for benzocaine and procaine are shown in Fig. 4. The data reported[1] on the aniline molecule have also been included for purposes of comparison. The quantum number for the inversion vibration, ν_i, is given at the left of each line; the wavenumber (cm^{-1}) above the ground state is given at the right. All transitions marked by arrows were observed, and the transition wavenumbers are indicated. The broken arrow represents a predicted frequency.

The ν_i = 0–1, 1–2, 0–2 and 2–3 transitions were identified in the spectrum of Fig. 3. In these transitions, the 0–1 and 2–3 generally appear in

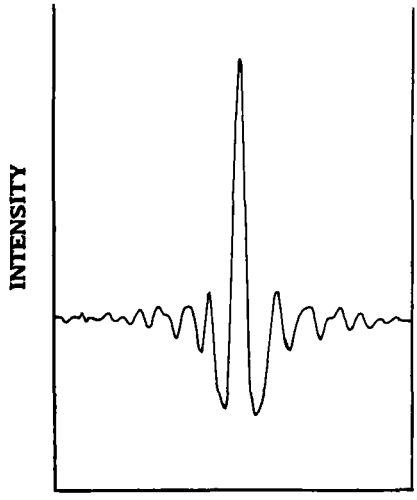

Fig. 2. Interferogram of reference in the 200-500 cm^{-1} range.

the spectra as bands of weak intensity, while the 1→2, 0→2 are identified as strong intensity bands. Thus the $\nu_i = 0 \rightarrow 1$ transition (ν_i being the quantum number for the inversion vibration) of PRC was observed at 43 cm^{-1} with weak intensity, as the 2→3 transition at ca. 374 cm^{-1}, while 1→2 and 0→2 appear with strong intensity at 510 and 551 cm^{-1}, respectively. The average deviation between the observed energy levels was less than 5 %. The energy levels in the inversion vibration of the amino group are very sensitive to the arrangement of the electrons in the molecule. Therefore, from the energy levels, the barrier to inversion may be calculated quite accurately.

The spectra also contained two bands of similar appearance at 407 and 322 cm^{-1}, which were identified as originating from the torsion plus and minus the inversion motions, $[\nu_\tau + \nu_{i(0\text{-}1)}]$ and $[\nu_\tau - \nu_{i(0\text{-}1)}]$ respectively, in complete analogy with aniline[1]. The computed frequency of torsional motion was 364.5 cm^{-1}, and the wavenumber of the 0→1 transition was 42.5 cm^{-1}. These values are in accordance with the pattern of inversion transitions shown in Fig. 4. The values reported for aniline[1] were $\nu_\tau = 277$ cm^{-1} and $\nu_{i(0\text{-}1)} = 69$ cm^{-1}.

The data reported for the FTIR spectrum of the vapour phase of aniline[1] and the solid state of benzoic acid[16] were used in the assignments of the other bands detected in the spectrum. The frequencies and intensities computed by AM1 were also utilized in the characterization of all the vibrations. The scale

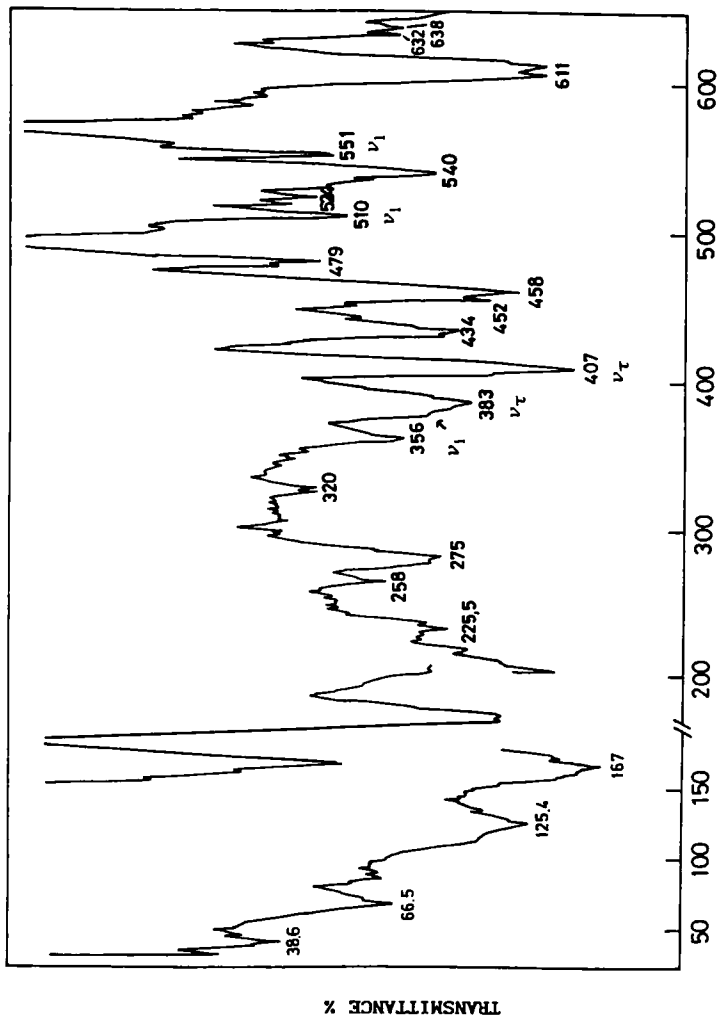

Fig. 3. FTIR spectrum of procaine in a polyethylene pellet.

Table 1. Fundamental frequencies for procaine calculated and observed experimentally by IR and Raman spectroscopy.

Calculated by AM1			Experimental		Characterization
Frequency (cm^{-1})	Relative intensity (%)[a]	Scaled frequency[b]	Far-infrared	Raman	
21 (17)	21		20 w		$\tau(NH_2\text{-ring-COO-}CH_2)^d + \tau(\text{-}CH_2\text{-}CH_3)$
27	21		38.5 m		$\tau(\text{-}CH_2\text{-}CH_3)$
47 (42)	27		43 vw		$\tau(NH_2)+\tau(\text{ring})^d + \tau^m(COO\text{-}CH_2\text{-}CH_2\text{-})^d + \Gamma(\text{-}CH_2\text{-}CH_3)$
51 (60)	29		66.5 m		$\Gamma(NH_2\text{-ring-COO-}CH_2\text{-})^d + \gamma(\text{C-H})$ in $\text{-}CH_2\text{-}CH_3$
80 (84)	25		83.5 vw	115 vw	$\gamma'(NH_2\text{-ring})^d + \tau(COO\text{-}CH_2)^d + \Gamma(\text{-}CH_2\text{-}CH_3)^*$
134 (129)	28		125.4 m		$\Gamma(\text{-}CH_2\text{-}CH_3)^d + \gamma(\text{C-N})$ as tertiary $+ \Gamma(NH_2\text{-ring})^{*d}$
182 (184)	18		167 s	182 w	$\tau(CH_3)$
221 (141)	35		225.5 w	225 vw	$\gamma'(NH_2\text{-ring-COO-}CH_2)^d$
280	39	270[c]	275 s	273.5 vw	10b, $\gamma(CCC) + \gamma(NH_2) + \gamma(COO)$
295 (299)	12		258 w		$\gamma(\text{C-N})$ as tertiary $+\gamma(\text{C-C})$ in $CH_2\text{-}CH_3 + \gamma(\text{-}CH_2\text{-}CH_3)^*$
322 (316)	32		322 w		$\gamma(\text{C=O}) + \gamma(\text{C-N})$ as tertiary $+ \gamma(\text{-}CH_2\text{-}CH_3)^*$
333 (322)	41	392	383 s, 407 vs?	401 w	$\tau(NH_2)$ torsion
358 (378)	50		320 w	300.5 m	$\Gamma(COO\text{-}CH_2\text{-}CH_2)^d + \Gamma(NH_2\text{-ring})^{*d} + \gamma(\text{C-N})^*$ as tertiary
379	22	407	434 m		16a, $\gamma(CCC) + \tau(NH_2)$ torsion
420 (390)	42		356 m	338.5 vw	$\Gamma(\text{-}CH_2\text{-}CH_3)^d + \gamma(\text{-}CH_2\text{-}CH_3)^*$
444 (431)	38		374 sh	414 vw	$\Gamma(NH_2)^d + \Gamma(\text{ring})^d + \Gamma(COO\text{-}CH_2\text{-}CH_2)^d$
			452 s, 458 vs		
466 (458)	84	498	479 vw, 510 s	496.5 w	$\gamma(NH_2)$ wagging $+ \Gamma[CH_2\text{-N-}(CH_2\text{-}CH_3)_2] + \Gamma(\text{ring})^{*d}$
473	100	586	551 s		$\gamma(NH_2)$ wagging
505	49	510	524 w	519 vw	16b, $\gamma(CCC)$
532 (525)	44				$\Gamma(\text{ring})^d + \Gamma(NH_2)^d + \Gamma(COO)^d + \delta(CCN)$ as tertiary
545 (549)	40		540 vs	536 vw	$\Gamma(CCOO) + \delta(CCN)$ as tertiary $+ \Gamma(\text{ring})^{*d}$
622 (650)	45		611 vs		$\delta(\text{C-N})$ as tertiary $+ \Delta_s(COO) + \Gamma(\text{C-H})$ in CH_3
668	40	625	632 w	622 m	6a, $\delta(CCC) + \Delta_s(COOC) + \Delta_s(CCO)$
679 (677)	30	640[c]	638 w	639 s	6b, $\delta(CCC) + \delta_s(CCOO) + \delta(NH_2)$

Abbreviations: s, strong; m, medium; w, weak; vw, very weak. [a]Related to the line computed at 473 cm^{-1}. [b]With scale factors for liquid benzene[14]. [c]With the scale factors for *p*-aminobenzoic acid[14]. [d]According to ref. 15. [*]Weak contribution.

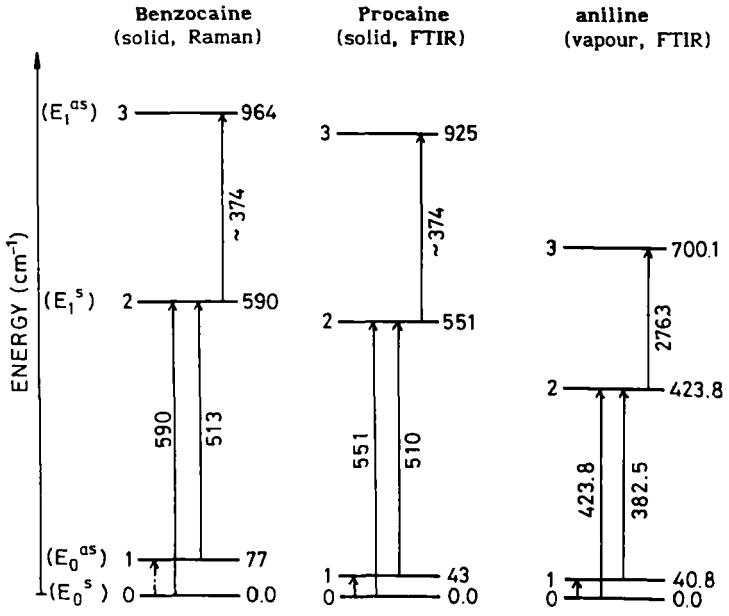

Fig. 4. Scheme of the inversion energy levels for the benzocaine, procaine and aniline.

factors obtained[14] for the ring modes in benzene and *p*-aminobenzoic acid, were used to correct the deficiencies in the AM1 semiempirical method. The ring vibrations were numbered according to Wilson's notation[17,18].

Raman spectra were also obtained for a clearer identification of the *p*-amino inversion transitions. Thus, Fig. 5 contains the low-frequency Raman features of solid PRC. The fifth column of Table 1 lists the lines registered and their assignments are given in the sixth column.

The Raman spectrum for the benzocaine molecule between 100-600 cm^{-1} is given in Fig. 6. The bands recorded in the infrared and Raman spectra are listed in the fourth and fifth columns of Table 2. The frequencies and relative intensities calculated by AM1 appear in the first and second columns. An analysis similar to that carried out on solid procaine culminated in calculation of the inversion energy levels of Fig. 4. The values are very close to those determined for procaine. Thus, the $\psi_o^s \rightarrow \psi_1^s$ and $\psi_o^{as} \rightarrow \psi_1^s$ transitions in the Raman spectrum, were at 590 and 513 cm^{-1}, respectively. The $\tau(NH_2)$ mode, $\nu_\tau + \nu_{i(0-1)}$, was detected at 406 cm^{-1}, close to the value for procaine, which confirms our assignations.

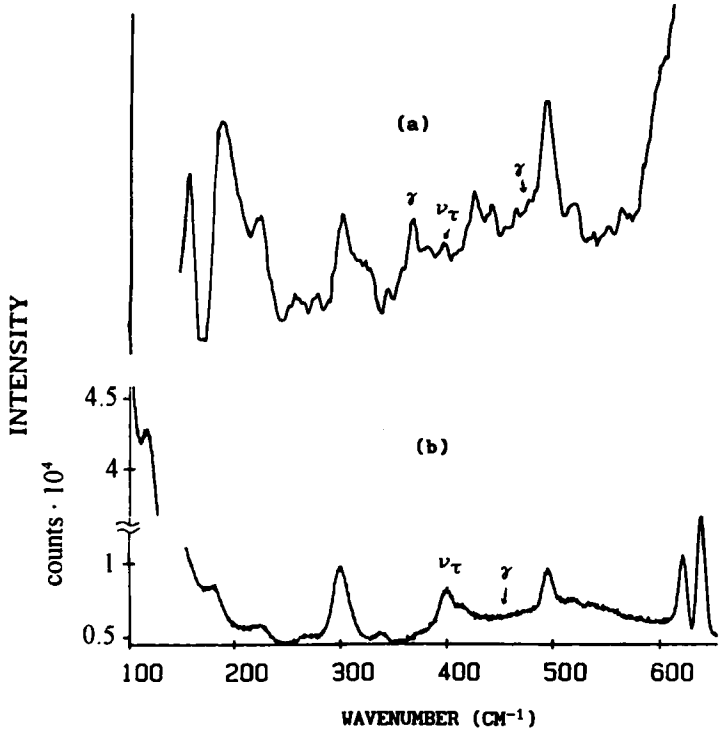

Fig. 5. Raman spectra for procaine in the solid state: a) 200 mω krypton laser, slits = 900 mic., 1K. b) 300 mω argon laser, 514.5 nm, slits = 400 mic.

Description of the torsion-inversion potential functions: The starting geometry for the calculations was taken from the crystal data[19-21], optimizing all the geometric parameters with the AM1 and CNDO/2 semiempirical methods, and at the 6-31G* ab initio level. The results for the NH_2 group of BEN are listed in Table 3, where ω is the inversion angle and ε is the *tilt* angle between the C-N bond and the aromatic ring plane (Fig. 7). A detailed study was previously carried out on both angles[9]. The results for PRC were very close to those for benzocaine, the fifth column of Table 3.

As a first step in the study of the torsion-inversion motion, the variation in ω with different torsional angles α (from 0-90°) was obtained (Figs. 8,9). The optimized values are given in Table 4. Since the differences in the *p*-amino group in the BEN and PRC molecules are small, the values in Figures

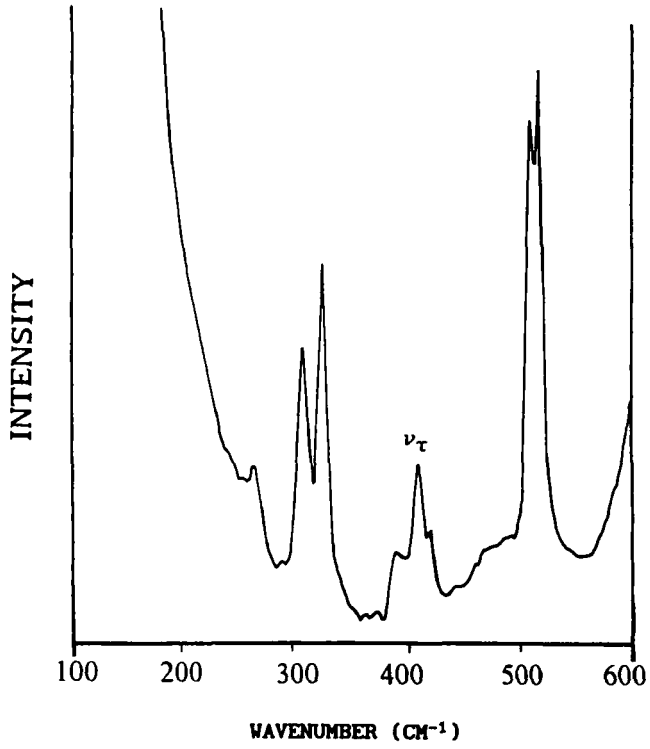

Fig. 6. Raman spectrum of benzocaine in the solid state using a 100 mω argon laser, slits = 300 mic., 3K.

8- 13 and Tables 4-5 are applicable to both molecules. Figs. 8,9 show an increase in ω with the torsional angle α, with a maximum value of 59.15° at α=90°. The geometric change in the NH_2 group with α results in a variation in the torsional constant, B_o. The calculated values of B_o for several angles α are shown in Table 4.

Deuteration of the compounds[22] produced the H→D isotope shift in the *p*-amino moiety, appearing -NHD and -ND_2 groups. The ∠HNH angle obtained using the Linnett equations[23] changed in the process, ∠HNH: 111.33° and ∠DND: 118.72°; calculating different values of B_o with the NHD and ND_2 groups (Table 4). Theoretical values of B_o calculated with inertial considerations[9] are also included in the Table. The results computed by AM1 and CNDO/2 were very similar.

Table 2. Fundamental frequencies of benzocaine calculated and observed by IR and Raman spectroscopy.

Calculated by AM1			Experimental		Characterization
Frequency (cm^{-1})	Relative intensity (%)[a]	Scaled frequency[b]	Infrared	Raman	
30	0				$\tau(NH_2\text{-ring})^d + \gamma(CH_2\text{-}CH_3)$
59	0				$\tau'(OO\text{-}CH_2\text{-}CH_3)^d$
76	0	69			$\tau(CH_2\text{-}CH_3)$ + 11, γ(C-H) ?
100	1				$\Gamma(\text{ring-}NH_2)^d + \Gamma(CH_2\text{-}CH_3)$
112	0			107 w	$\tau(CH_3)$
150	1			142 w	$\tau(\text{-}CH_2\text{-O-}) + \tau(CH_3)$
				240 vw	$\gamma(NH_2)$ wagging
261	2		318 w	322 m	$\Gamma(\text{ring-}NH_2)^d + \Gamma(CH_2\text{-}CH_3)$
				306 m	$2[\tau(\text{-}CH_2\text{-O-}) + \tau(CH_3)]$
280	2	266		261 vw	10b, γ(C-H)
320	3	378[c]	390 m	406 w	$\tau(NH_2)$ torsion
354	4		360 m[f]		$\Gamma(NH_2\text{-ring})^d + \Gamma'(CH_2\text{-}CH_3)^d$
379	0	407		418 vw	16a, γ(CCC)
408	6	397		390 vw[f]	15, δ(C-H) + $\Gamma(CH_2\text{-}CH_3)^d$
440	1				$\Gamma(NH_2) + \Gamma(\text{COO-ring})^d + \Gamma(CH_2\text{-}CH_3)$
476	100		518 vw	513 m	$\gamma(NH_2)$ wagging
		576[c]	590 m	590 sh	$\gamma(NH_2)$ wagging
506	8	543	510 w	507 m	16b, γ(CCC)
535	6				$\Gamma(NH_2) + \Gamma(\text{ring})^d + \Gamma(CH_2\text{-}CH_3)^d$

Abbreviations: s, strong; m, medium; w, weak; vw, very weak; sh, shoulder. [a]Related to line computed at 476 cm^{-1}. [b]With the scale factors for liquid benzene[14]. [c]With the scale factors for *p*-aminobenzoic acid[14]. [d]According to ref. 15. [f]In solution.

Table 3. Optimized bond lengths in Å and bond angles in degrees obtained using different quantum chemical procedures.

Parameter	Benzocaine			Procaine
	AM1	6-31G*	CNDO/2	AM1
r C-N	1.3880	1.3647	1.39	1.3876
r N-H	0.9931	0.9918	1.07	0.9930
∠ HNH	115.19	117.66	107	115.29
∠ HNC	116.21	121.17	111.5	116.28
ω	34.50	0.88	51.8	34.17
ε	2.86	0.75	3.6	2.83

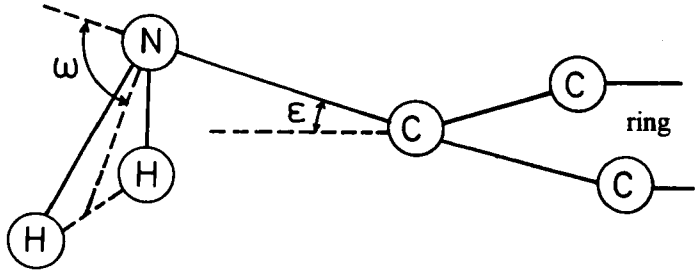

Fig. 7. Description of the ε and ω angles.

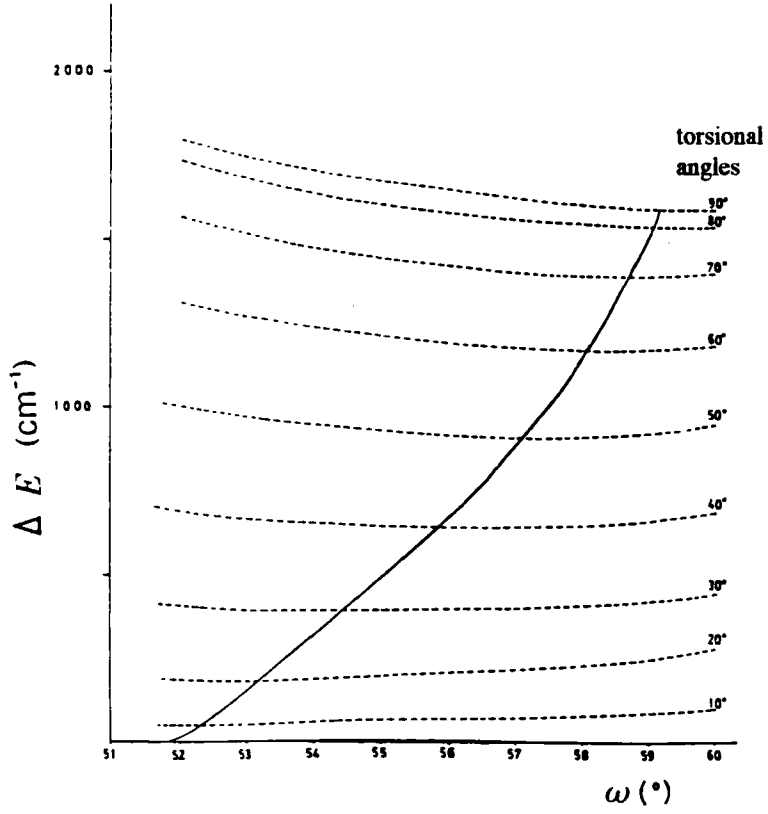

Fig. 8. (....) Energy curves for different torsion (α) and inversion angles (ω).
(__) Geometric minimum of the curves.

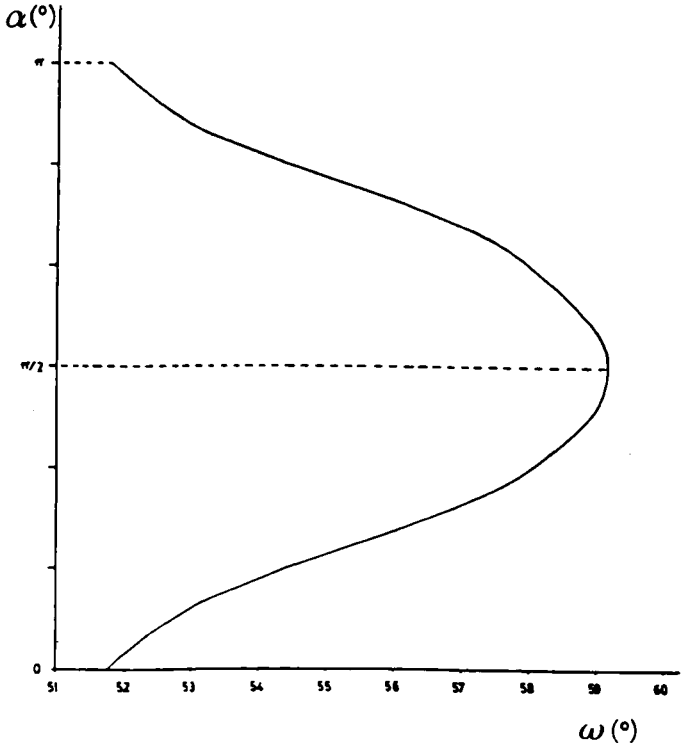

Fig. 9. Different optimum inversion angles (ω) in a torsion of 180°.

Table 4. Optimum inversion angles (ω) and torsional force constants (B_o).

Parameters	Torsional angles			
	α= 0°	α= 30°	α= 60°	α= 90°
Optimum inversion angle ω(°)	51.8	54.4	58.0	59.15
B_o (cm^{-1}) -NH_2	8.84	8.71	8.52	8.47
-NHD	6.01	5.91	5.79	5.75
-ND_2	4.55	4.48	4.38	4.35
-NH_2*	8.83	8.70	8.51	8.46
-NHD*	6.01	5.93	5.81	5.77
-ND_2*	4.58	4.51	4.42	4.40

*Calculated based on inertial considerations[8].

The torsion-inversion potential function was plotted with the minimum energies determined for the different torsional angles (Fig. 10). The barrier height, 1587.05 cm^{-1}, was appreciably lower than in simple torsion, 1795 cm^{-1} with $\varepsilon \neq 0$. The form of the curve in Fig. 10 is not exactly fitted to an analytical function of the simple form[24] $V(\alpha) = V_2 (1 - \cos 2\alpha)/2$. Instead, the Fourier expansion $V(\alpha) = \Sigma V_n (1-\cos n\alpha)/2$ should be used. Setting n = 2, 4, 6, and 8 yields the V_n values 1580.87, -26.85, 6.18, and 8.54, respectively.

In the torsional potential function, the frequencies are sometimes calculated[5] using the barrier height (V_2), and B_o. Two methods were used: For the harmonic approximation (AA), the torsional frequency is given by $\nu_\tau^{AA} = (B_o \sum_n n^2 V_n)^{1/2}$, the seventh column of Table 5. For n = 2, the equation is reduced to $\nu_\tau^{AA}(V_2) = 2\sqrt{B_o V_2}$, values of the sixth column.

The second method solves the hindered-rotation Hamiltonian (RH)[25,26]

$$H = -\frac{d}{d\alpha} B \frac{d}{d\alpha} + \frac{1}{2} V_n^{eff}(1 - \cos n\alpha)$$

where $V_n^{eff} = V_n + V_n^{pseudopot.}$. $V_n^{pseudopot.}$ arises from the trigonometric expansion of various kinetic terms[25]. Note that the geometry of the rotor was theoretically optimized for each rotation angle, so that in order to calculate the rotation constant (B), we used the expression: $B = B_o + \sum_n B_n (1-\cos n\alpha)/2$. Substituting n = 0, 2, 4, 6 in the expansion in trigonometric series of B, yielded the coefficients of the force constant in Table 5. These values were substituted in the Hamiltonian to compute the torsional energy levels, plotted in Fig. 10 for the NH_2 group, with a broken line for the *sine* symmetry and a solid line for the *cosine* symmetry. The 0→1 transition gave the frequencies of the eighth $\nu_\tau^{RH}(V_2)$ and ninth columns $\nu_\tau^{RH}(\Sigma V_n)$ in Table 5. However, the frequency values were close to those calculated by (AA), a simpler method. $\tau(NH_2)$ was calculated by AM1 at 320 cm^{-1} for BEN and 333 cm^{-1} for PRC.

Applying the geometric parameters assumed for the present compounds yielded the relation $[B_o(NH_2)/B_o(ND_2)]^{1/2} \cong 1.39$. Since the electronic properties ought to be invariant for isotopic exchange, the value of V_2 is conserved on H-D exchange. Therefore the values of the $\tau(NH_2)/\tau(ND_2)$ relationship were 1.395 for (AA) and 1.375 for (RH). This relationship is very useful in identifying of the torsional bands in the spectra of deuterated samples, because their values are close to those experimentally observed. Thus, the Raman spectrum value for BEN in the solid state was 1.526, while the infrared and Raman spectrum values for PRC were 1.429 and 1.548, respectively.

Fig. 11 plots the frequencies of the first three torsional transitions (ν_{ij} in cm^{-1}), 0-1, 1-2, and 2-3, versus the barrier height (V_2 in cm^{-1}), for the

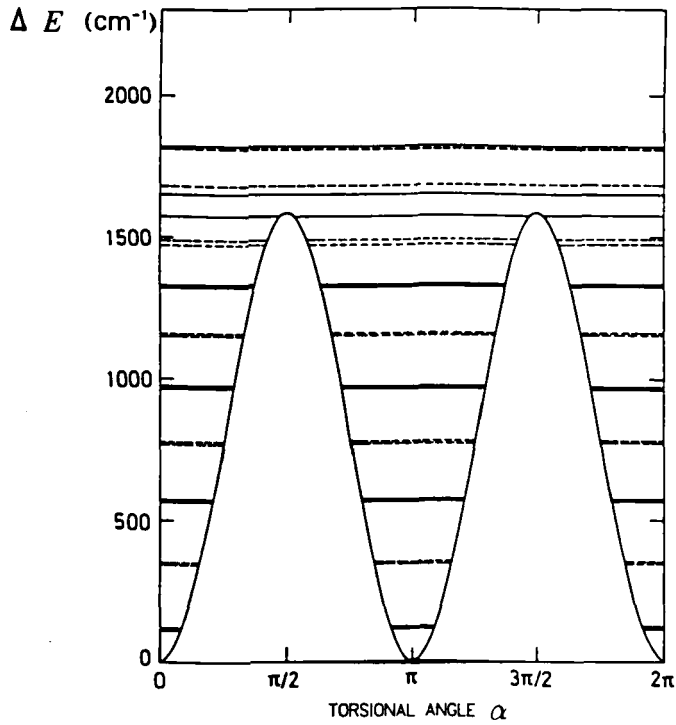

Fig. 10. Torsional potential function obtained by minimizing the energy with respect to ω at each point. Energy levels were calculated for -NH_2 with a torsional Hamiltonian.

Table 5. Coefficients in the trigonometric expansion of B_α in cm^{-1} (n=0,2,4,6); torsional frequencies in cm^{-1} obtained by a harmonic approximation (AA) and a torsional Hamiltonian (RH).

p-amino group	n				ν_τ^{AA}		ν_τ^{RH}	
	0	2	4	6	V_2	ΣV_n	V_2	ΣV_n
- NH_2	8.84	-0.37	-0.05	-0.004	237	243	223	221
- NHD	6.01	-0.25	-0.04	-0.003	195	200	185	184
- ND_2	4.55	-0.19	-0.03	-0.002	170	174	162	161

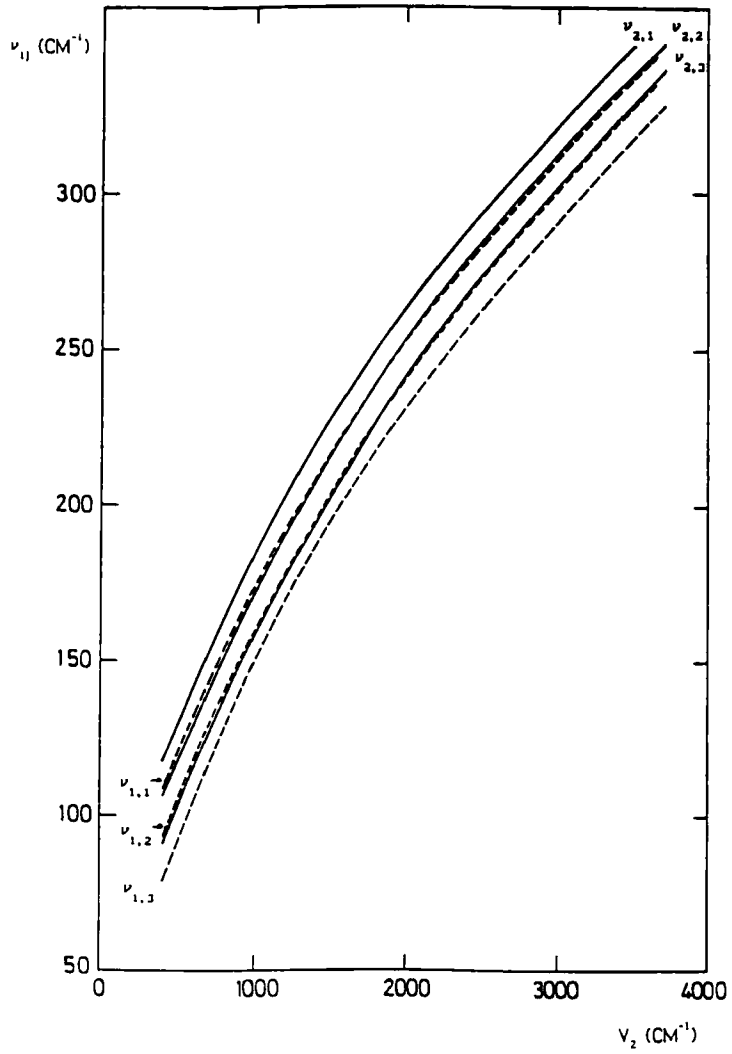

Fig. 11. Curves for the determination of all torsional transitions between the first three energy levels for the -NH_2 group.

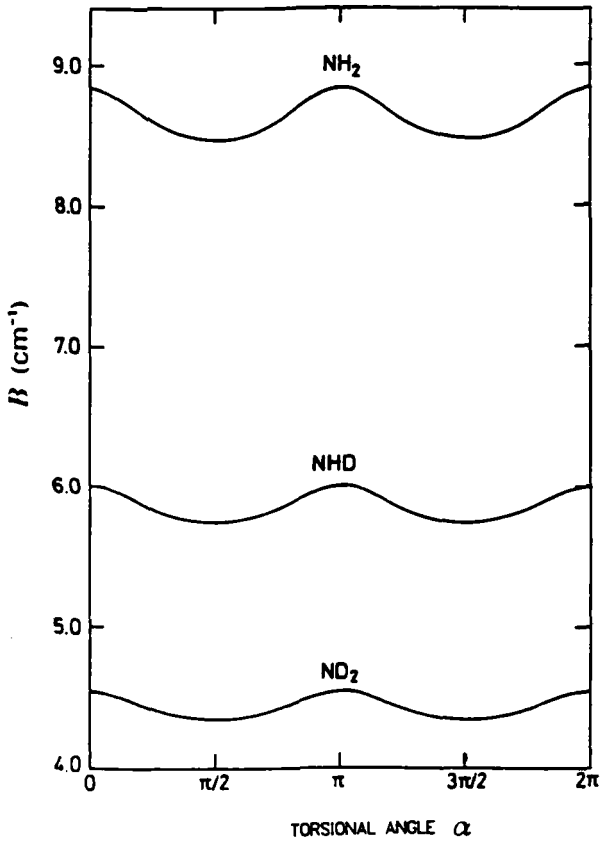

Fig. 12. Torsion-inversion constant force, B_o, versus torsional angle, α.

NH_2 group with $\alpha = 0°$ (B_o=8.47 cm^{-1} and $\nu_{1,1}$, $\nu_{1,2}$, $\nu_{1,3}$) and $\alpha = 90°$ (B_o=9.37 cm^{-1} and $\nu_{2,1}$, $\nu_{2,2}$, $\nu_{2,3}$). Using this Figure, the value of V_2 can be found if the value of ν_{ij} is known, and vice-versa. Fig. 12 represents the variation of B_o with the value of the angle α for the torsion-inversion motion of the -NH_2, NHD and ND_2 groups.

Changes in the amino group structure on rotation and inversion were also quite marked, with alterations in N-H bond lengths, ∠CNH and ∠HNH angles all showing the most stable pyramidal form to be intermediate spacing between the planar (most - conjugated) and the rotated (least -conjugated)

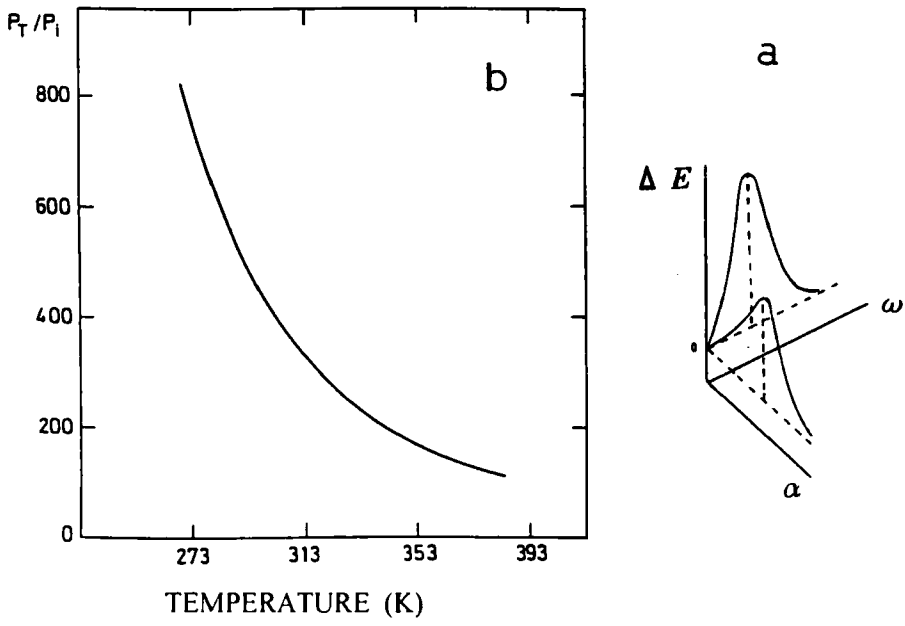

Fig. 13. a) Diagram of the probability of torsion or inversion in the hydrogens of the *p*-amino group; b) plot of torsion/inversion probabilities on temperature.

conformations. The angle changes are, in fact, so large as to correspond to nearly pure sp^2 hybridization in the completely planar case and essentially sp^3 hybridization in the rotated pyramidal form.

Influence of temperature: All FTIR bands showed comparable relative frequency shifts with temperature, large changes without discontinuities. This also applied to the band widths. The relationship of probabilities between the electronic populations in the torsion and inversion motions was studied in relation to temperature (Fig. 13). The probability of torsion (P_τ) in the hydrogen atoms of the $-NH_2$ group is $P_\tau \sim exp\,(-E_\tau/KT)$, where E_τ is the barrier height[9] in the torsion (cm^{-1}) and T is the temperature in Kelvin. Analogously, the probability of inversion is $P_i \sim exp\,(-E_i/KT)$, where E_i is the barrier height in the inversion (cm^{-1}). These equations were used to establish the relationship $P_\tau/P_i = \exp\,[(E_i-E_\tau)/KT]$ and to plot Fig. 13b. The probability of inversion motion increased as temperature rose.

CONCLUSIONS

The present FTIR spectra of PRC showed several lines caused by transitions in the inversion vibration of the *p*-amino group and permitted observation and characterization of the torsion modes. Information on the full set of vibrations, especially those in the low-wavenumber region, will help overcome the shortage of data from which the present compounds suffer. In the torsional motion of the amino group, the inversion angle (ω) was observed to increase from torsional angle α=0° to the maximum value at α=90°, resulting in a change in the torsional constant, B_o.

The torsional frequencies observed in the far-infrared spectra were similar the theoretical calculations for both molecules.

As sample temperature rose, the probability of inversion motion over torsion motion increased. The calculations were in agreement with the observed results in the spectra, which showed a decrease in the torsional band and an increase in the wagging band as temperature increased.

ACKNOWLEDGEMENTS

The authors wish to thank C. Sigüenza for her help with the experimental measurements. The spectra were recorded at the Molecular Spectra Laboratory of the "Daza de Valdes" Optics Institute (CSIC) in Madrid.

REFERENCES

1. R.A. Kydd and P.J. Krueger, *Chem. Phys. Letters*, **49**, 3 (1977); *J. Chem. Phys.* **69**, 2 (1978).
2. N.W. Larsen, E.L. Hansen, and F.M. Nicolaisen, *Chem. Phys. Letts.*, **43**, 3, 584 (1976).
3. M. Remko and P.T. Van Duijnen, *J. Mol. Struct.*, **104**, 451 (1983).
4. P.O. Dideberg, J. Lamotte, and L. Dupont, *Acta Crystallog.*, **B36**, 1500 (1980).
5. M. Alcolea Palafox, *Spectrochim. Acta*, **44A**, 12, 1465 (1988).
6. G.R. Freeman and C.E. Bugg, *Acta Crystallog.*, **B31**, 96 (1975).
7. M. Alcolea Palafox, *Indian J. Pure & Appl. Phys.*, **3-4**, 5842 (1991).
8. M. Alcolea Palafox, *J. Mol. Struct.*, **175**, 81 (1988).
9. M. Alcolea Palafox, *Rev. Roum. Chim.*, **34**, 8, 1667 (1989).

10. M.J.S. Dewar, E.G. Zoebisch, E.F. Healy, and J.J.P. Stewart, *J. Am. Chem. Soc.*, **107**, 3902 (1985).

11. (a) D.A. Liotard, E.F. Healy, J.M. Ruiz, and M.J.S. Dewar, in R.D. Dennington, II and E.F. Healy (Eds.), *AMPAC MANUAL. Version 2.1. A General Molecular Orbital Package*, Univ. of Texas at Austin, USA (1989). (b) M.J.S. Dewar and J.J.P. Stewart, *Q.C.P.E. Bull.* **6**, 506 (1986).

12. M. J. Frisch, G.W. Trucks, M. Head-Gordon, P.M.W. Gill, M. W. Wong, J.B. Foresman, B. G. Johnson, H. B. Schlegel, M. A. Robb, E. S. Replogle, R. Gomperts, J. L. Andres, K. Raghavachari, J. S. Binkley, C. Gonzalez, R. L. Martin, D. J. Fox, D. J. Defress, J. Baker, J. J. P. Stewart, and J. A. Pople, *GAUSSIAN 92*, Gaussian Inc., Pittsburgh PA, 1992.

13. N. Müller and A. Falk, *BALL AND STICK Program*, Version 2.2r4, Austria, 1981-89.

14. M. Alcolea Palafox, *in preparation*.

15. M. Alcolea Palafox, *J. Mol. Struct. (Theochem.)*, **236**, 161 (1991).

16. H.R. Zelsmann and Z. Mielke, *Chem. Phys. Letters*, **186**, 6 (1991).

17. E.B. Wilson, *Phys. Rev.*, **45**, 706 (1934).

18. G. Varsanyi, *Assignments for Vibrational Spectra of Seven Hundred Benzene Derivatives*, vol. 1, Adam Hilger, London, 1974.

19. T.F. Lai and R.E. Marsh, *Acta Crystallog.*, **22**, 885 (1967).

20. S. Kashino, M. Ikeda, and M. Haisa, *Acta Crystallog.*, **B38**, 1868 (1982).

21. B.K. Sinha and V. Pattabhi, *Proc. Indian Acad. Sci. (Chem. Sci.)*, **98**, 3, 229 (1987).

22. M. Alcolea Palafox, *Spectrosc. Letters*, **27**, 5, 613 (1994); *J. Raman Spectrosc.*, **20**, 765 (1989).

23. D. Lin-Vien, N.B. Colthup, W.G. Fateley, and J.G. Grasselli, *The Handbook of Infrared and Raman Characteristic Frequencies of Organic Molecules*, Ed. Academic Press Inc., San Diego, California, USA (1991).

24. J.D. Lewis, T.D. Malloy, J.R. Tainer, T.H. Chao, and J. Laane, *J. Mol. Struct.*, **12**, 427 (1972).

25. A. Brauler, E. Mathier, R. Meyr, M. Ribeaud, and H.H. Gunthard, *Mol. Phys.*, **15**, 597 (1968).

26. M. Onda, T. Motoda, and I. Yamaguchi, *Bull. Chem. Soc. Jpn.*, **58**, 242 (1985).

Date Received:December 12, 1996
Date Accepted: June 13, 1997